



In-Situ CO₂ Partitioning Measurements in a *Phragmites australis* Wetland: Understanding Carbon Loss through Ecosystem Respiration

Xueyang Yu^{1,2} · Siyuan Ye^{1,2,3}  · Linda Olsson^{4,5} · Mengjie Wei^{1,2} · Hans Brix^{4,5}

Received: 19 February 2020 / Accepted: 24 May 2020
© Society of Wetland Scientists 2020

Abstract

Common reed (*Phragmites australis*) is dominant vegetation of temperate coastal wetlands in northeast China. To studying the link between ecosystem respiration (R_{eco}) and its influential factors, a multi-year in-situ experiment was carried out in a newly restored wetland during the growing seasons of 2012 to 2014. Total in-situ R_{eco} was separated into soil microbial and below-ground root respiration (R_{s+r}) and plant respiration (R_{plant}). The soil microbial respiration rate (R_s) was isolated from R_{s+r} , making it easier to understand each component of R_{eco} . With the wetland restoration process, the seasonal average aboveground biomass (dry mass) increased from 411.5 g m⁻² to 2048.1 g m⁻² and the corresponding R_{eco} increased from 751.78 mg CO₂ m⁻² h⁻¹ to 2612.41 mg CO₂ m⁻² h⁻¹. R_{plant} contributed averagely 69% ~ 71% to R_{eco} on the whole seasonal scale and the plant activity was strongly seasonal. With 1 g of aboveground common reed biomass (dry weight), approximately 3.6 mg CO₂ would be produced per hour during the sprouting period while it could be as low as 0.3 mg CO₂ during plant senescence period. Inundation regime dominated the contribution of R_s to R_{eco} and the flooded contribution would lower the R_s contribution to as low as 11%.

Keywords Coastal wetland · Soil respiration · Plant respiration · Field observation · Carbon cycling

Introduction

Since the industrial revolution in 1880s, the atmospheric CO₂ concentration has increased from 270.8 ppm to 390.5 ppm and is currently increasing at a rate of approximately 2.0 ppm yr⁻¹ (Ciais et al. 2013). Regarded as the

highest contributor to the anthropogenic greenhouse effect, CO₂ represents the main atmospheric phase of the global carbon cycle (Rodhe 1990; Archer 2010). Covering approximately 5 ~ 8% of all land surface, wetlands are estimated to store more than 30% of the world's soil carbon (Mitsch and Gosselink 2007). As an ecotone of terrestrial and aquatic system, wetlands are more sensitive to anthropogenic force as well as natural impact such as climate change (Moomaw et al. 2018; Huang et al. 2020). It is concerned that the great storage of carbon may potentially exacerbate the increase of atmospheric CO₂ concentration, which leads to greater greenhouse effect and higher surface temperature (Updegraff et al. 2001; Ma et al. 2019).

The common reed (*Phragmites australis* Cav. Trin ex Steud) wetlands are worldly spread and are most productive among all wetland types (Brix et al. 2001). The Liaohe Delta owns the largest reed wetland in the world with a total area of approximately 800 km². Reed is the raw material for local paper industry there. The reed wetlands were managed to be more productive, so that the demand of pulp production can be satisfied. The harvest of reeds may alter the natural carbon cycling and has potential feedbacks to climate change when

✉ Siyuan Ye
siyuanye@hotmail.com

¹ Key Laboratory of Coastal Wetland Biogeosciences, China Geological Survey, Qingdao Institute of Marine Geology, Qingdao 266071, China

² Laboratory for Marine Geology, Qingdao National Laboratory for Marine Science and Technology, Qingdao 266061, China

³ Qingdao Institute of Marine Geology, China Geological Survey, MLR, 62 Fuzhou Road, Qingdao, China

⁴ Department of Bioscience, Aarhus University, 8000C Aarhus, Denmark

⁵ Sino-Danish Centre for Education and Research, 8000C Aarhus, Denmark

400,000 metric tons of reed biomass were harvested annually to paper production (Brix et al. 2014).

The continuous measurement of CO₂ exchange between the atmosphere and the wetland ecosystem has been studied. As a carbon sink, wetlands can sequester 41 ~ 144 g C m⁻² yr⁻¹ (Zhou et al. 2009). However, some studies believe the common reed wetland can convert to carbon source and emit as much as 97 g C m⁻² yr⁻¹ (Nieveen et al. 2010). The gaseous absorption and emission of CO₂ determined the role that an ecosystem plays in carbon cycle. As main CO₂ source, respiration is one of the key processes. The ecosystem emission of CO₂ can be divided into two components (Unger 2008). On one hand, the CO₂ emitted from soil surface is the product of heterotrophic respiration and plant root respiration (Hanson et al. 2000). On the other hand, autotrophic respiration, which was originated from aboveground vegetation, also contributes to ecosystem respiration (Berglund et al. 2011). Because of interannual difference of precipitation (Haverd et al. 2017), solar radiation, temperatures (Lee et al. 2015), plant phenology and hydrological regimes (Juszczak et al. 2013), it is hard to clarify whether a wetland is a carbon sink or a carbon source only if the influence of those biotic and abiotic factors were figured out.

Ecosystem respiration in coastal wetlands are influenced by lots of environmental factors including temperatures (Juszczak et al. 2013; Arora et al. 2016), soil properties (Hassink 1992), plant types (Xu et al. 2014) and soil hydrological conditions (Guan et al. 2011; Bai et al. 2020). Linked with each other, the environmental factors, especially the meteorological factors, keep changing diurnal and seasonal, which crates bias on evaluating the combined influence of the changing environment (White et al. 2014; Marínmuñiz et al. 2015). Specially, plant and microbial respiration have difference in response to temperature and water level change (Dawson and Tu 2009; Hall and Hopkins 2015; Wu et al. 2017). During the growing season, autotrophic respiration could be as important as heterotrophic respiration while during non-growing season, soil heterotrophic respiration dominates the ecosystem respiration, which, added to the difficulties of evaluating carbon budget of wetlands.

Common reed is a perennial vascular plant that grows in wetlands, which can tolerate salinities up to 20‰ (Achenbach et al. 2013), and the aerenchyma provides pathway for directly gaseous transportation from the air to the root (Kim et al. 1999). The oxygen could reach the rhizosphere, and greenhouse gas such as CO₂ and CH₄ could be transported upwards. It is reported that more than 70% of methane was emitted by plant-mediated transport due to the absence of methanotrophic (Miao et al. 2012). Reed could grow more than 3 m high, making it hard to measure the ecosystem respiration directly by the traditional chamber method. Although eddy covariance method provides net ecosystem exchange rates, the ecosystem respiration rates estimated via empirical

models. Some studies have managed to observe ecosystem respiration directly. Hu et al. (2014) found less than 20 mg CO₂ m⁻² h⁻¹ could be transported from the underground part. Yang et al. (2017) conducted a five-day continuous chamber measurement that reveals the diurnal variation of common reed net ecosystem exchange of CO₂. However, in-situ chamber study of reed wetland respiration is rare, and partitioning ecosystem CO₂ emission into different components are needed to understand the contribution of plant and soil to ecosystem respiration.

The in-situ chamber method was applied to study the entire ecosystem CO₂ emission from a reed wetland in the Liaohe River delta. In order to figure out the source of CO₂ and comparing the amount from different part of the ecosystem, extra measurements were conducted after handling processes of in-situ common reeds. Together with the biomass and environmental variables we recorded, the specific controlling factors for separated part were extracted. Then we integrated our findings to a fast assessment method to evaluate the ecosystem CO₂ emission.

Materials and Methods

Study Area

This study was conducted in the Liaohe Delta (121°25′–123°31′ E, 40°39′–41°27′ N) of Northeast China (Fig. 1). Natural wetlands in the Liaohe Delta cover about 2610 km², which account for about 69% of the delta area (Ji et al. 2009). In addition, rice agriculture (non-natural wetlands) comprises approximately 3287 km², and is spread in the Liaohe Delta. The Liaohe Delta is located in the temperate continental monsoon zone with mean air temperature of 8.3 °C, and a mean annual precipitation of 612 mm with most rainfall occurring in summer. The mean annual evaporation rate is 1705 mm, and the mean annual sunshine duration is approximately 2769 h (Luo et al. 2003). The average tidal range in the area is 2.7 m; tides are semi-diurnal. The Liaohe Delta comprises what is believed to be the largest reed (*Phragmites australis* Cav. Trin ex Steud) wetland in the world with a total area of approximately 800 km² (Brix et al. 2014). Our study site was a newly restored wetland vegetated by *Phragmites australis*, located at 36°04′33″N, 122°23′33″E. The site was covered by water for most mid-summer and the average height of plant was approximately 1.5 m.

The soil on the study sites is a silty clay loam with a sand, silt and clay content of 20%, 65% and 15%, respectively, and a soil bulk density of approximately 1.21 g cm³. The soil total and organic carbon content are low, averaging 19.7 g kg⁻¹ and 18.9 g kg⁻¹, respectively, and total nitrogen content is 1.9 g kg⁻¹. Soil pH is 7.2 ± 0.3 (std. dev.) and soil pore water salinity is 1.9 ± 0.4‰.

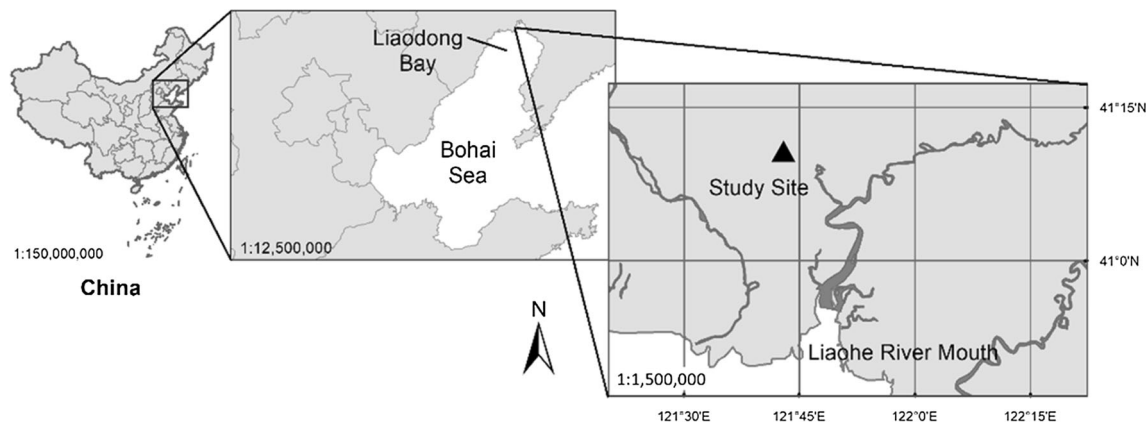


Fig. 1 The location of the study site in the Liaohé Delta, Northeast China

CO₂ Flux Measurements

CO₂ fluxes were measured using a field-portable infrared gas analyzer (Li-8100A, LI-COR Biosciences, Inc., Lincoln, NE, U.S.A.) with a commercial survey dark chamber (8100–103). CO₂ measuring range was 0 to 3000 ppm with errors less than 1.5%. Circular survey collars (10 cm tall by 20 cm diameter) were inserted 3 to 5 cm into the soil 2 h before measurement began to limit the influences of recent disturbance. The survey collar measured an area of 318 cm². The total volume of the flux chamber was calculated as the sum of the volume of the commercial survey chamber system (~4843 cm³) plus the volume inside the collar factoring insertion depth of each collar individually. CO₂ concentrations were recorded at 1 Hz during 90 s measurement periods, and individual flux rates were the average of two measurements per chamber conducted in immediate series (10 s apart; 90 s each) to ensure similarity over at least two cycles (Mukhopadhyay and Maiti 2014). Prior to each field trip, the infrared gas analyzer was calibrated and checked for zero drift using CO₂-free nitrogen gas (Dyukarev 2017).

CO₂ fluxes (F , mg CO₂ m⁻² h⁻¹) were calculated according to the following equation:

$$F = \frac{dc}{dt} \frac{M}{V_0} \frac{P}{P_0} \frac{T_0}{T} \frac{V}{S}$$

Where dc/dt (mol h⁻¹) is the slope of the linear regression line for CO₂ concentration over time before chamber saturation; M (mg mol⁻¹) is the molecular mass of CO₂; P (in kPa) is the barometric pressure; T (in Kelvin) is the absolute temperature during sampling; V (in Liters) is the total volume of the enclosure measuring space; S (in m²) is the ground area of the dark chamber. Finally, V_0 (22.4 L/mol), T_0 (273.15 K) and P_0 (101.3 kPa) are the gas mole volume, absolute air temperature, and atmospheric pressure under standard conditions for gas, respectively (Song et al. 2009).

Experimental Design

Fluxes of CO₂ were measured approximately monthly during the growing seasons of 2012, 2013, and 2014 (Fig. 2), for a total of 13 months of measurements over the 3 years. Soils of Liaohé Delta wetlands are frozen to depths of 15 cm during the months of December to March (Ye et al. 2016). Six plots were established, and all had different amounts of vegetation coverage in each observation month. The measurements were performed during 10:00 to 14:00 under full sunlight (Table 1). On each plot, four measuring procedures were included, as follows:

- (1) Measurement of ecosystem respiratory CO₂ flux by including all vegetation and soil area through the use of a dark chamber that prevents photosynthesis, defined as “ R_{eco} ”;
- (2) Measurement of plant material after cutting and removing all *P. australis* vegetation at 1 to 2 cm above the soil surface (or 1 to 2 cm above the surface water level when inundated) (Fig. 2). Placing all detached *P. australis* into another sealed dark survey collar that prevents photosynthesis immediately after harvest (within 2 min), then the CO₂ flux inside the sealed chamber was tested, and the flux was defined as R_{plant} ;
- (3) Measurement of soil CO₂ flux within the processed survey chamber after the plant removal, which was defined as R_{s+r} . R_{s+r} measured soil microbial respiration plus respiration of live roots underlying those soils, when soils were not inundated, and measured the CO₂ efflux from water surface plus the CO₂ came out of the stems left in survey collar, when the soils were inundated.
- (4) The remaining stems of *P. australis* were sealed by cutting below water level during inundated periods, or by filling toothpaste during unflooded periods after the R_{s+r} was measured (Fig. 2). Then the soil CO₂ flux within the survey chamber was measured again to avoid the influence of plant intermediate gas transport. This flux item was defined as R_s .

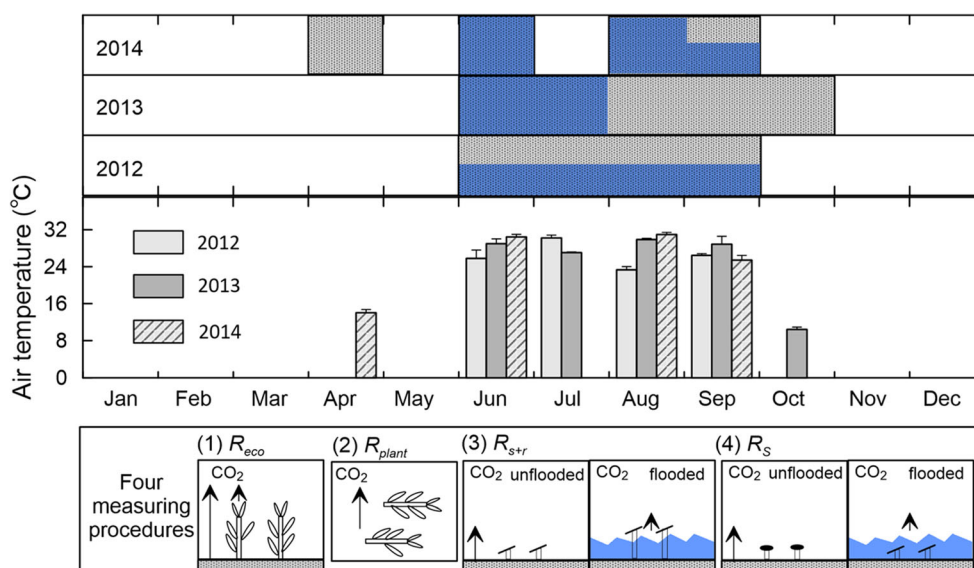


Fig. 2 Observation period and procedures from 2012 to 2014. Observation periods are marked as filled grey patches, and vertical blue patches indicate the relative water level of a corresponding observation period. Months with continuous blue rectangles refer to inundation of all six plots; months half covered in blue rectangles refer to inundation of only some of the plots. Lack of blue rectangles equates to no inundation. Experimental procedures (R_{eco} , R_{s+r} , R_{plant} , and additional fluxes) are re-

iterated visually on the bottom panel. The R_{eco} measures the ecosystem respiration, which contains the plant respiration and soil respiration; The R_{plant} is the measured respiration on the plant material after cutting within 2 min; The R_{s+r} measures the soil respiration and the root respiration; The additional measurement is designed to quantify CO_2 emitted from the plant stems

Apart from the observed fluxes above, respiration of other components could be calculated. R_r , calculated as $R_{s+r} - R_s$, was defined as the CO_2 efflux transported by reed stems, indicating the amount of root respiration. Moreover, we combined the fluxes to represent contributions of different part to whole ecosystem respirations.

Biomass Measurements

All harvested *P. australis* plant materials were dried to a constant mass at 65 °C in a convection oven for estimation of

Table 1 Measuring date of the three growing seasons

Year	Month	Day	Julian day
2012	6	8	160
2012	7	5	187
2012	8	12	225
2012	9	6	250
2013	6	17	168
2013	7	23	204
2013	8	22	234
2013	9	21	264
2013	10	15	288
2014	4	17	107
2014	6	24	175
2014	8	2	214
2014	9	25	268

aboveground biomass (*AGB*). A 30 cm deep surface soil sample was taken within each survey collar after CO_2 flux measurements were completed during each sampling period. Living roots of *P. australis* were collected in the core, separated from the soil column and dried at 65 °C to constant mass to measure belowground biomass (*BGB*).

Statistical Analysis and Modeling

All monthly data are presented as arithmetic means among plots with corresponding standard errors among plots. Correlation analyses were conducted using SPSS v20.0 to examine the relationships between the fluxes and the measured environmental variables. In all tests, the differences were considered significant at $p < 0.05$. Least square curve fitting was applied using Grapher v10.0 (Golden Software, Golden, CO, U.S.A.) to quantify the influence of environmental factors.

Results

Biomass

Both above ground biomass (*AGB*) and belowground biomass (*BGB*) within survey collars increased consistently during the 3 years (Fig. 3). The average total biomass in 2012, 2013 and 2014 were 411.5 g m⁻², 1362.3 g m⁻² and 2048.1 g m⁻²,

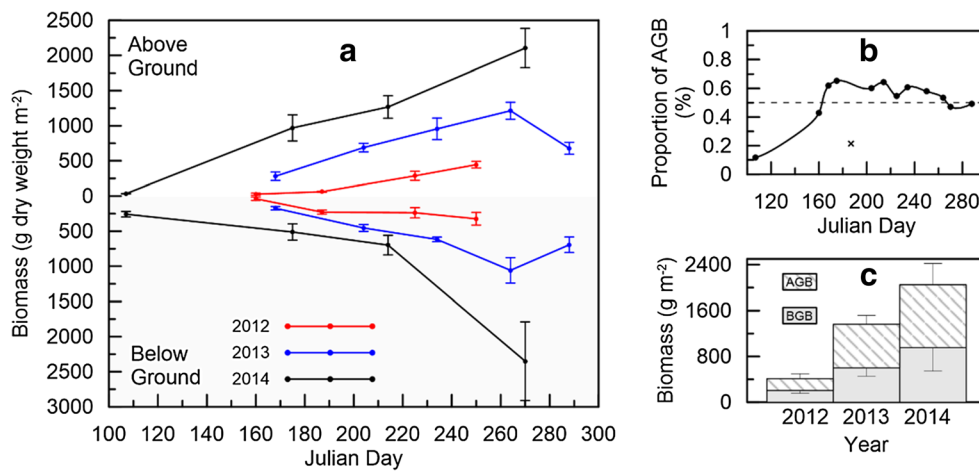


Fig. 3 Seasonal variation of both aboveground and belowground biomass during the observation periods. **a** The error bars are the standard error of the mean biomass. **b** The proportion of aboveground biomass (*AGB*) indicates the ratio of *AGB* to total biomass, which also

had seasonal variation. The cross point was not included in the spline smoothing. **c** The interannual variation of biomass. Bars represent the annual average biomass and error bars represent the standard error of the mean value

respectively. The increase rate of total biomass dropped from 231% to 50%. As a restored wetland, this indicated the increase of annual gross primary productivity and the wetland become more and more natural. The average accumulation rate of *AGB* and *BGB* in 2012 were $4.8 \text{ g m}^{-2} \text{ day}^{-1}$ and $2.7 \text{ g m}^{-2} \text{ day}^{-1}$, respectively. During the restoration process, reed grows better in 2013, with the accumulation rate of *AGB* and *BGB* of $9.7 \text{ g m}^{-2} \text{ day}^{-1}$ and $8.8 \text{ g m}^{-2} \text{ day}^{-1}$. Finally, in the year of 2014, the *AGB* and *BGB* accumulation rates were $12.4 \text{ g m}^{-2} \text{ day}^{-1}$ and $12.1 \text{ g m}^{-2} \text{ day}^{-1}$, which was higher than the other 2 years.

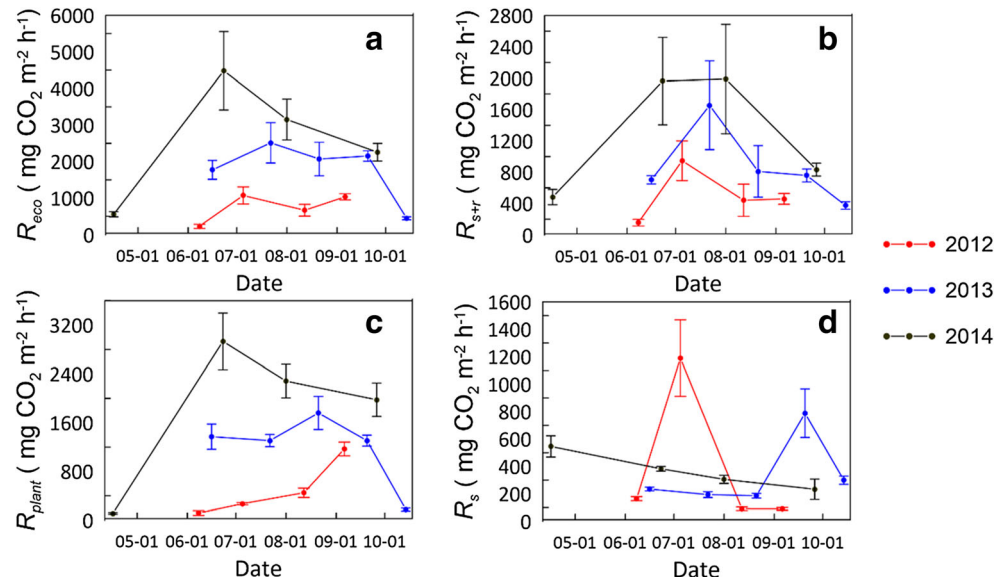
However, surface soil total carbon content showed no increase trends, with the average of $2.45 \pm 0.96\%$, $1.25 \pm 0.32\%$ and $1.71 \pm 1.37\%$ in the three consecutive years. Seasonally, both *AGB* and *BGB* kept increasing during the growing

seasons. In 2013, both *AGB* and *BGB* decreased compared to their previous observations. Biomass dropped at the end of the growing seasons due to the plant senescence and biomass allocation. During the beginning of the growing seasons, the *AGB* increased with higher speed than that of *BGB*, noting that the proportion of *AGB* to total biomass increased from 0.12 to 0.65. After the common reeds were fully developed in July, the ratio decreased to 0.47 at the end of growing season. The averaged *AGB* proportion was 0.5 within our survey collars.

The Observed Fluxes

Mean ecosystem respiration (R_{eco}) in June, 2012 was the lowest during all observing periods (Fig. 4a), the average ecosystem respiration rate was $3.36 \pm 54.51 \text{ mg CO}_2 \text{ m}^{-2} \text{ h}^{-1}$, while

Fig. 4 The observed greenhouse gas exchange in the growing seasons of 2012, 2013 and 2014. The greenhouse gas exchange of the three growing seasons was plotted red, blue and black, respectively. Error bars indicate standard error of the mean within each data group. **a** Seasonal variation of ecosystem respiration (R_{eco}). **b** Seasonal variation of soil and root respiration (R_{s+r}). **c** Seasonal variation of plant respiration (R_{plant}). **d** Seasonal variation of soil respiration (R_s)



the largest ecosystem respiration occurred in June, 2014, which was as high as $4484.17 \pm 1070.74 \text{ mg CO}_2 \text{ m}^{-2} \text{ h}^{-1}$. Seasonally, R_{eco} effluxes in July were higher than that of other months in both 2012 and 2013, while they were not tested in 2014. The R_{eco} tended to peak at mid-summer when both temperature and plant activity were the highest of a growing season. The seasonal average of R_{eco} kept increasing from $751.78 \text{ mg CO}_2 \text{ m}^{-2} \text{ h}^{-1}$ (year 2012) to $2612.41 \text{ mg CO}_2 \text{ m}^{-2} \text{ h}^{-1}$ (year 2014) during the three observing years.

The R_{s+r} has similar seasonal trend as R_{eco} , peaking at July, and the average R_{s+r} increased from $947.0 \pm 253.5 \text{ mg CO}_2 \text{ m}^{-2} \text{ h}^{-1}$ in 2012 to $1655.1 \pm 566.0 \text{ mg CO}_2 \text{ m}^{-2} \text{ h}^{-1}$ in 2013 (Fig. 4b). The highest R_{s+r} was $1989.2 \pm 697.7 \text{ mg CO}_2 \text{ m}^{-2} \text{ h}^{-1}$ in August 2014, peaking later than 2012 and 2013. The R_{s+r} of June 2014 was $1963.7 \pm 558.0 \text{ mg CO}_2 \text{ m}^{-2} \text{ h}^{-1}$, and has no significant difference with that of August 2014 ($p > 0.05$). The seasonal mean R_{s+r} was continuously increasing in the three growing seasons, as R_{eco} did. Both R_{eco} and R_{s+r} exhibited unimodal distribution at seasonal scale. The interannual variation of R_{s+r} was similar with R_{eco} and has increasing patterns within each separated month.

Unlike the other 2 years, R_{plant} kept increasing from June to September in 2012, and ranged from $118.8 \text{ mg CO}_2 \text{ m}^{-2} \text{ h}^{-1}$ to $1168.8 \text{ mg CO}_2 \text{ m}^{-2} \text{ h}^{-1}$ (Fig. 4c). As the observation site was restored in 2012, it was likely that the plant did not grow well just after the wetland restoration, leading to the unique seasonal R_{plant} pattern in 2012. Except for 2012, the R_{plant} had seasonal unimodal distribution and in the year 2013 and 2014, it peaked in August and June, respectively. The average R_{plant} kept increasing from $501.5 \text{ mg CO}_2 \text{ m}^{-2} \text{ h}^{-1}$ to $1826.6 \text{ mg CO}_2 \text{ m}^{-2} \text{ h}^{-1}$ during the three growing seasons, which meant that the reeds grew better in the consecutive growing seasons.

R_s , however, kept as low as $91\text{--}546 \text{ mg CO}_2 \text{ m}^{-2} \text{ h}^{-1}$ during most observing periods (Fig. 4d), indicating less contribution to ecosystem respiration, except for July 2012, when R_s had no significant difference with the corresponding R_{eco} ($p > 0.05$). This also happened in April 2014. In these 2 months, low R_{plant} (less than $300 \text{ mg CO}_2 \text{ m}^{-2} \text{ h}^{-1}$) were observed when the soil was not flooded and was drier compared to other observing periods. In 2014, the R_s had a decreasing seasonal pattern. If the data of July 2014 and September 2013 were ignored, the seasonal trend of the other 2 years were also decreasing. R_s also had interannual variation if the spikes were ignored, like R_{eco} , R_{s+r} and R_{plant} , R_s kept increasing since 2012, from $115.8 \text{ mg CO}_2 \text{ m}^{-2} \text{ h}^{-1}$ in 2012 to $367.1 \text{ mg CO}_2 \text{ m}^{-2} \text{ h}^{-1}$ in 2014.

The Calculated Flux

As was shown in Fig. 5, similar with R_{plant} , the R_r also peaked in summer except for 2012, exhibiting a seasonal unimodal distribution. The interannual variation was also similar to the observed fluxes, exhibiting a continuously increasing pattern.

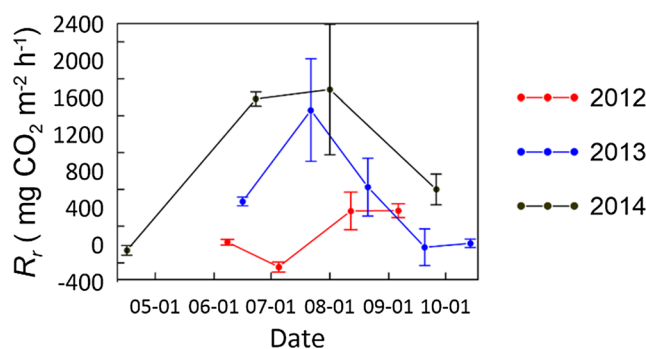


Fig. 5 The calculated root respiration (R_r) in the growing seasons of 2012, 2013 and 2014. The greenhouse gas exchange of the three growing seasons was plotted red, blue and black, respectively. Error bars indicate standard error of the mean within each data group

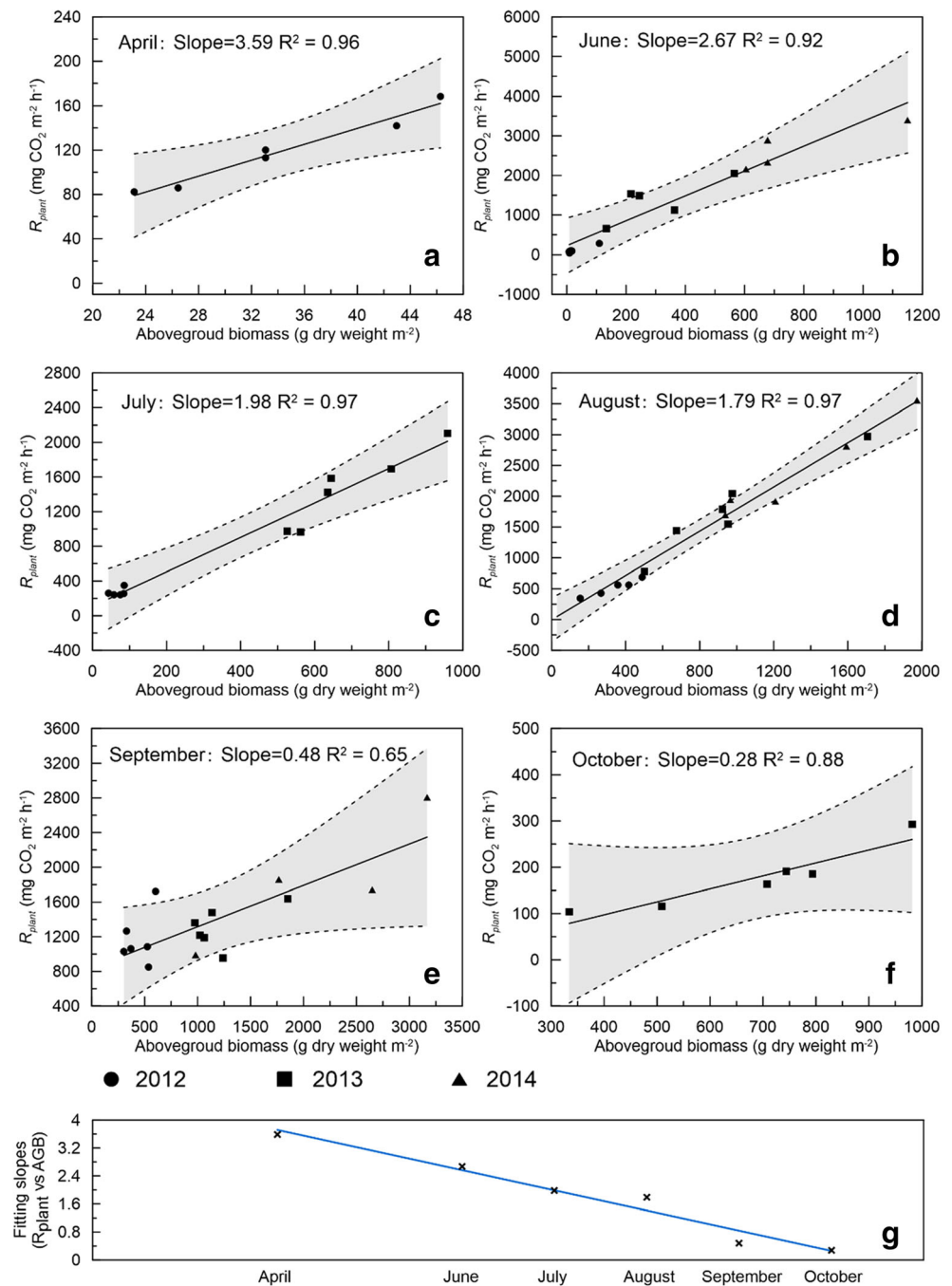
The seasonal average R_r of 2012, 2013 and 2014 was from $128.9 \text{ mg CO}_2 \text{ m}^{-2} \text{ h}^{-1}$, $507.3 \text{ mg CO}_2 \text{ m}^{-2} \text{ h}^{-1}$ and $949.9 \text{ mg CO}_2 \text{ m}^{-2} \text{ h}^{-1}$, respectively. In 2014, the R_r reached $1683.5 \pm 707.7 \text{ mg CO}_2 \text{ m}^{-2} \text{ h}^{-1}$ in early August of 2014. During summer time, the R_r were high deviated, indicating great spatial variations.

Relationships between the Plant Respiration and Biomass

The relationships between R_{plant} and AGB seemed to be the most straightforward. As was acknowledged, more biomass led to more respiration. Instead of putting all R_{plant} and AGB observations together, to demonstrate this seasonal variation of plant CO_2 respiration ability for a certain amount, linear regression was conducted using the biomass and R_{plant} data in each separated month (Fig. 6). As was shown, the R_{plant} was significantly correlated with AGB . As an indicator of plant activity, the slope of the linear regression decreased from April to October (Fig. 6g), indicating that reed reached the highest plant activity at the early stage of growing, not in mid-summer. According to our results, 1 g dry AGB could respire as much as $3.59 \text{ mg CO}_2 \text{ h}^{-1}$ in the early growing stage (April). But in the end of growing season (October), 1 g dry biomass dry AGB could respire as less as $0.28 \text{ mg CO}_2 \text{ h}^{-1}$, which was equal to 7.8% of the highest plant respiration activity.

R_r demonstrated the convective flow from the stems after the plants were removed. As a kind of vascular plant, the developed aerenchyma made it possible for *P. australis* to transport CO_2 generated by roots (Brix et al. 1996; Armstrong and Armstrong 2010). Shown in Fig. 7, the calculated fluxes R_r had significant linear correlation with AGB , regardless of the low fitting goodness. No significant relationship was detected between R_r and the BGB , which was likely due to the spatial variance of root biomass distribution (Engloner 2009; Wang et al. 2018). The AGB , positively correlated with BGB , could work as a proxy to estimate the CO_2 transportation when the aboveground part was removed. The

Fig. 6 The relationship between plant respiration (R_{plant}) and aboveground biomass (AGB) in **a** April, **b** June, **c** July, **d** August, **e** September and **f** October. Fluxes observed in the growing season of 2012, 2013 and 2014 are marked with circles, squares and triangles, respectively. The grey backgrounds in subplot **a** to **g** indicate the 99.99% confidence interval of each fitting, meaning that the data point outside this range is very likely outliers and thus are not included in the fittings. **g** The slope of each month fitting was extracted and plotted versus datetime, which displays significant ($p < 0.01$) seasonal decreasing trend



influencing factors was not limited to the AGB, as the main roots of *P. australis* were linked belowground, and the inundation regime, plant growing stage and the root morphology could also influence the CO_2 transportation.

The influences of environmental factors on respiration rate of other ecosystem parts were more complicated, because the respiration was influenced by several factors at the same time. The interactions would cover up real relationships if all R_{eco} or R_{s+r} data were put together. Therefore, further efforts were needed to separately analyze the impact of temperature as well as hydrological conditions.

Discussions

Seasonal Constitution of the Ecosystem Respiration

Except for the inundation regime, other factors related to seasonal variation, such as temperature change and plant growing stage, could also influence the constitution of R_{eco} (Han et al. 2012). The plant kept growing during the growing seasons and was regarded the dominant part of wetland ecosystem respiration during mid-summer and was believed contributed most to the whole R_{eco} (Hirota et al.

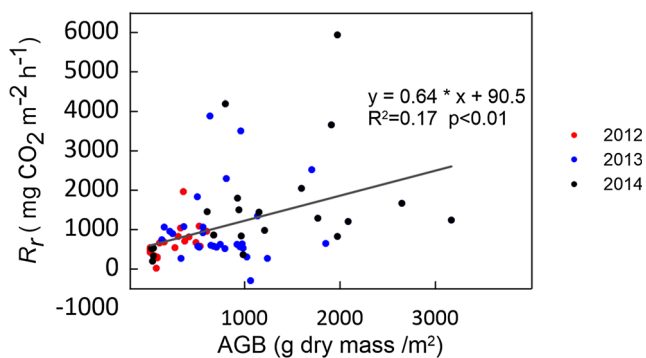
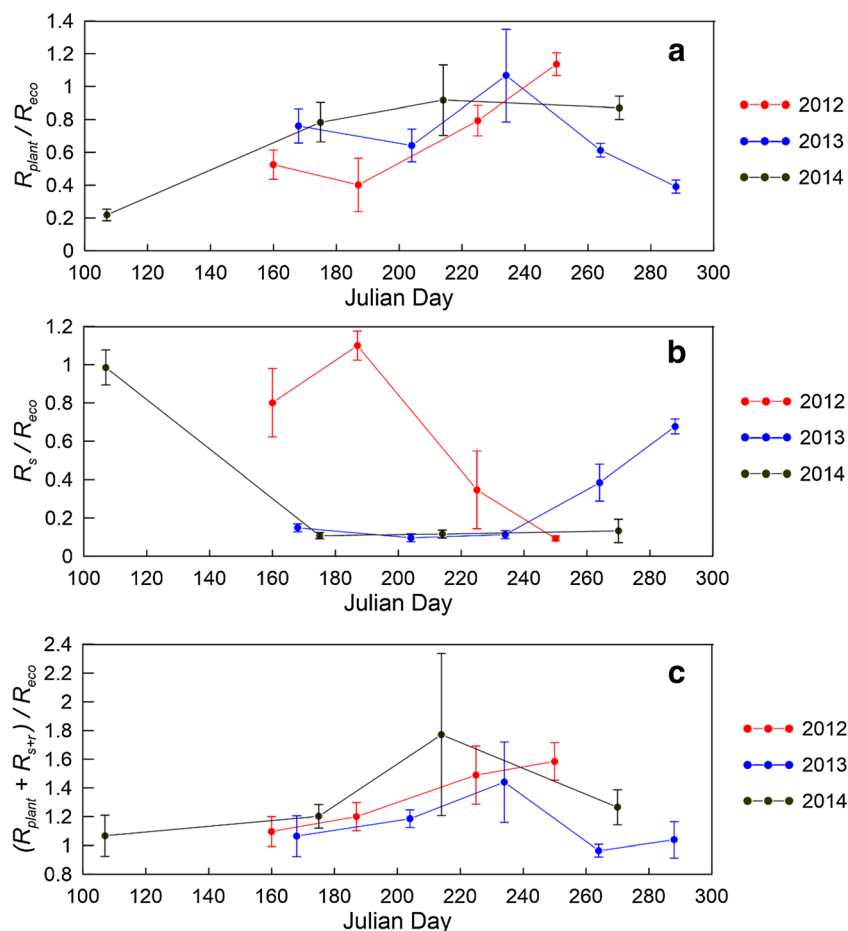


Fig. 7 The relationship between root respiration (R_r) and aboveground biomass (AGB). The 2012, 2013 and 2014 growing season data were colored red, blue and black, respectively. All data points were included in the linear fitting

2006). Here, the R_{plant}/R_{eco} ratio indicated the proportion of plant respiration to total ecosystem respiration. During the beginning and the end of growing seasons, this ratio tended to be lower than that of mid-summer when above 80% ecosystem respiration was derived from plant (Fig. 8). The average contribution of R_{plant} to R_{eco} in the three observation growing seasons was 69% ~ 71%. The lowest ratio occurred at April of 2012, which was 0.22. In

comparison, the R_s/R_{eco} kept low in mid-summer except for 2012, while in the beginning and the end of growing season, R_s/R_{eco} could be as high as 0.8, indicating that 80% ecosystem respiration was derived from soil heterotrophic respiration. Averagely, the R_s contributed 40% to ecosystem respiration, taking those high values into consideration. But R_s dominated ecosystem respiration only when low plant respiration occurred (Fig. 8). Similarly, the plant did not grow well in 2012 summer, making an increasing pattern of R_s/R_{eco} . Another reason of low R_s/R_{eco} was the regularly inundation in mid-summer. As described above, the flooded water restricted the gaseous transport between the atmosphere and the soil. The $(R_{plant} + R_{s+r})/R_{eco}$ indicated the change of ecosystem respiration capacity before and after the plants were detached. It was easier for gas to be transported both downwards and upwards after the plant was detached (Brix et al. 1996), making the sum of plant respiration, root respiration and the soil respiration averagely 27% higher than the measured ecosystem respiration. In reality, this ratio also had seasonal variations and it tended to be higher in late summer but kept low in the beginning and the end of growing season (Fig. 8c). In the August of 2019, due to the high R_r and decreasing R_{plant} ,

Fig. 8 Seasonal variation in the ratios of ecosystem respiration components to ecosystem respiration (R_{eco}). The error bars represent standard error of the mean value within each data group. **a** The ratio of plant respiration (R_{plant}) to R_{eco} . **b** The ratio of soil respiration (R_s) to R_{eco} . **c** The ratio of sum of ecosystem components ($R_{s+r} + R_{plant}$) to R_{eco}



the $(R_{plant} + R_{s+r})/R_{eco}$ peaked at 1.8, which meant 80% more CO_2 would be released if the plant was detached at this time.

The Influence of Inundation Regimes to R_s and the Constitution of Ecosystem Respiration

Water level was regarded the dominant factor in extreme moisture conditions such as desiccation and water logging, in the intermediate water table level, however, soil ecosystem respiration did not necessarily increase with deeper drainage (Berglund and Berglund 2011), this phenomenon also happened in our results. We found that the R_s decreased significantly during inundation periods. The R_s was mainly derived from the heterotrophic respiration, when the soil was flooded, the water worked as physical blocking of the gas transport from the soil to the atmosphere, which limited the oxygen availability of soil microbes on one hand, and preserve the CO_2 produced by soil microbes on the other hand (Pugh et al. 2018). It was reported that CO_2 efflux from soil is very sensitive to water level variations just around the soil surface (Lafleur et al. 2005). By comparing the contribution of each part of ecosystem, we could see that when the whole system was flooded, R_s contributed averagely 10.8% of R_{eco} , while during unflooded period, the R_s contributed averagely 67.8% of R_{eco} (Fig. 8a). This meant, compared to the rates of R_{plant} , the rate of gas exchange between the surface water and the atmosphere was relatively low in our study. Similarly, this finding indicated high potential ecosystem respiration derived from soil organic matters occurred only when soil was exposed directly to the air as gaseous oxygen was available. Although the oxygen could be dissolved in water, then utilized by soil microbes, the oxygen utilization speed and the efficiency were significantly decreased (Krauss et al. 2012) and this phenomenon has been documented previously for CH_4 (Devol et al. 1990). Moreover, when inundated, R_{plant} contributed averagely 69.1% to R_{eco} , and when the soil was not flooded, R_{plant} contributed 38.9% of R_{eco} (Fig. 8b), making the plant main source of CO_2 . These findings suggested that the soil respiration under inundation regime should be separately considered because the fluxes might not show any obvious patterns in correlation with environmental factors.

Moreover, the R_r/R_{eco} ratio indicated the contribution of plant-mediate transport of CO_2 fluxes, and further indicated the amount of root respiration, considering the test difference between R_{s+r} and R_s was merely whether the left stem was sealed or not. By comparing R_{s+r} and R_s , we could see the plant mediate transport of CO_2 could be equal to 31.1% of R_{eco} (Fig. 8c). When the soil was not flooded, the contribution of transport CO_2 to R_{eco} (equal to R_r/R_{eco} ratio) was not significantly different from 0.

This demonstrated that the plant-mediate CO_2 transport during unflooded period was not as high as that of flooding periods. By adding R_{s+r} and R_{plant} together, we could explore the influences of plant cutting to ecosystem respirations (Fig. 8d). Compared to R_{eco} , cutting resulted in extra 11%–14% (by median values) CO_2 emission both in flooded and unflooded condition. Under this, the inundation regime, however, has no significant difference. This suggested that if the reeds were cut or the reed shoot was damaged, more CO_2 emission occurred, which meant the harvest of reed for paper factory could potentially stress global warming by adding more CO_2 to the atmosphere.

The Determination of Plant Respiration

The *AGB* was a suitable proxy to evaluate the variation of plant respiration and further regulated the variability in R_{eco} (Wohlfahrt et al. 2008). However, Gao et al. (2017) found that R_{eco} did not have significant linear correlations with *AGB*, owing to the different plant growing stages. According to our results, R_{s+r} was close to R_{eco} in June and July of 2012 and in April of 2014. In other months, as described above, plant averagely contributed to 69.1% of R_{eco} during inundation and 38.9% during unflooded periods. This meant CO_2 derived from plant (autotrophic respiration) was higher than the CO_2 from soil surface (heterotrophic respiration). As was told in the results, R_{plant} stayed high in mid-summer, but kept low during the beginning and end of each growing season. This was believed the result of plant seasonal life cycles (Song and Liu 2016). We were acknowledged that biomass of reed kept increasing when they grew up, but more plant tissue did not necessarily result in higher plant respiration (Townsend et al. 2018). In other words, CO_2 derived from same amount of plant tissues (e.g. 1 g dry mass) during a certain period (e.g. 1 h) of different growing stage was not always the same. When plant started to senescence, the respiration rate for a certain amount of *AGB* slowed down. This meant the average plant respiration activity of one plant shoot kept decreasing during the reed growth. Knowing that, with the stems stretching, the stem biomass proportion kept increasing while the proportion of leaves kept dropping. The stems, however, respired slower than fresh leaves of same mass, resulting in the continuously dropping. The slopes were taken and plotted on seasonal scale, a linear regression could fit all point significantly, and the plant activity could be predicted. However, plant activities were linked to plant phenology and was influenced by environmental factors such as temperature and soil hydrological conditions (Liu et al. 2011). Here we just put all slopes together to explore the seasonal variation of plant respiration activity (the slope of R_{plant} versus *AGB*). As was

shown in Fig. 6, the slopes kept decreasing from 3.59 in April to 0.28 in October. With the reed growing and the biomass accumulation, more biomass was allocated to construct the plant structure, which led to the seasonal decreasing of the slope.

The Determination of Soil Respiration

Generally, soil respiration was regarded as temperature controlled processes (Suseela et al. 2015; Carey et al. 2016), as the soil CO₂ efflux was derived from heterotrophic respiration by microbes (Mäkiranta et al. 2009). Soil water regime, texture and organic matter the determination of microbial activities as they provided substrate and suitable external environment (Vargas and Allen 2008). As we described above, the inundation regime significantly influenced the ratio R_s/R_{eco} , which meant the relationship between R_s and temperature would be covered up if all flux data were included without separating different inundation regimes. R_s were divided into two groups according to the inundation regime. As was shown in Fig. 9, the R_s under flooded condition were generally lower than 400 mg CO₂ m⁻² h⁻¹ even with higher air temperatures. In reverse, R_s under unflooded condition had a wider air temperature range of 6~35 °C, but with less data, because the soil in summer time was regularly flooded. R_s of both groups had an exponential relationship with air temperature. The exponential fitting parameter of both groups were not alike.

For the temperature sensitivity parameter, it was 0.06 °C⁻¹ for unflooded group, and it was 0.16 °C⁻¹ for the flooded group, while the reference respiration parameter (respiration rate at 0 °C) was 170.6 mg CO₂ m⁻² h⁻¹ for unflooded condition, which was much higher than that of flooded condition (2.33 mg CO₂ m⁻² h⁻¹). Although both groups had a relatively low goodness of fit, both R² were lower than 0.65, the significance was lower than 0.01, indicating that the correlation was significant. By comparison, it was shown that the R_s under flooded condition was relatively lower within the whole temperature range (Fig. 10).

The Rapid Evaluation of Ecosystem Respiration in *P. australis* Wetlands

Figuring out the ecosystem respiration constitution of the *P. australis* wetlands, a rapid evaluation method could be made. By the discussion above, whole R_{eco} was interpreted as the sum of R_{plant} and R_{s+r} . In reality, this algorithm overestimated the ecosystem because the plants were detached when conducting the experiments. Here we added a conversion coefficient to rectify the overestimation. As was described in Fig. 8, the $(R_{plant} + R_{s+r})/R_{eco}$ kept stable and was independent of inundation regime change, we take the median value of 1.125 instead of the seasonal average value of 1.270, because the extreme values we observed created bias to estimation. Therefore, the in-situ ecosystem respiration could be interpreted as:

Fig. 9 The components of ecosystem respiration under flooded and unflooded regimes. The boxes indicate the lower and upper quartiles within each data group while the whiskers indicate the 5% and 95% percentile of each group. The line inside each box represents the median value within each group. Those dots are data outside 5%~95% percentile of data range. **a** The ratio of soil respiration (R_s) to ecosystem respiration (R_{eco}). **b** The ratio of plant respiration (R_{plant}) to R_{eco} . **c** The ratio of root respiration ($R_r = R_{s+r} - R_s$) to R_{eco} . **d** The ratio of sum of ecosystem components ($R_{s+r} + R_{plant}$) to R_{eco}

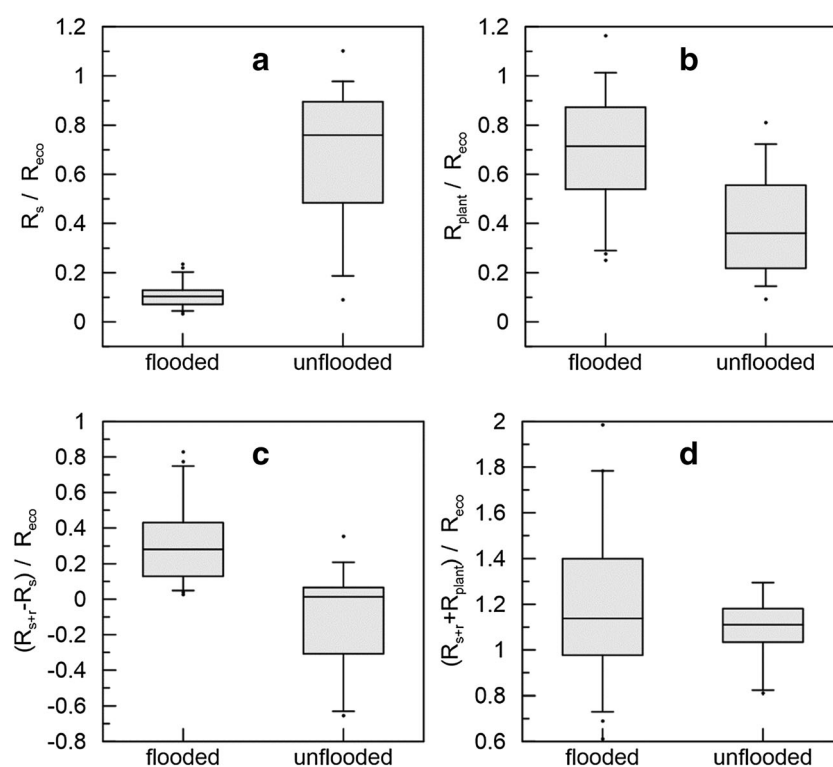
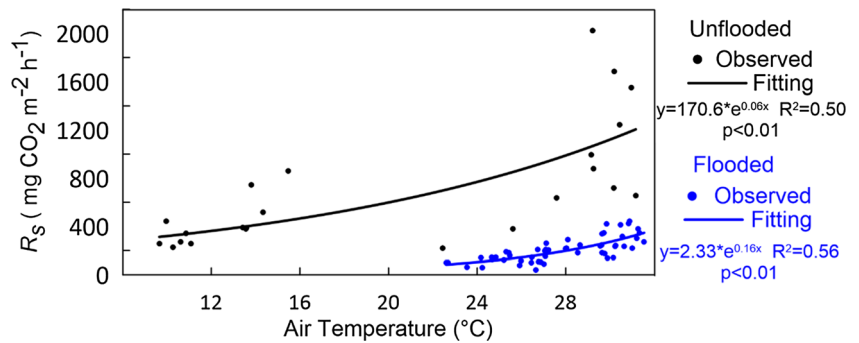


Fig. 10 The relationship between soil respiration (R_s) and air temperatures. Data are distinguished by inundation regimes. The R_s fluxes of unflooded condition are colored black while the R_s fluxes of flooded condition are colored blue



$$R_{eco} = (R_{plant} + R_{s+r})/1.125 \quad (1)$$

The R_{plant} was estimated via the relationship described in Fig. 6, and the AGB was used as driving variable:

$$R_{plant} = AGB \times a_{act} \quad (2)$$

where a_{act} was the plant respire ability in $\text{mg CO}_2 \text{ g}^{-1}$ dry plant mass h^{-1} . The seasonal variation of a_{act} was calculated by the correlation in Fig. 8 where the Julian day worked as a proxy (Fig. 11). Considering the real condition, the a_{act} was set within the range of 0.25 ~ 3.6 $\text{mg CO}_2 \text{ g}^{-1}$ dry plant mass h^{-1} , all value exceeded this range was set to the nearest limit manually.

The R_{s+r} was calculated by the sum of R_s and R_r :

$$R_{s+r} = R_s + R_r \quad (3)$$

where R_s was calculated according to the temperature response relationship described in Fig. 10, which was:

$$R_s = \begin{cases} 170.6 \times e^{0.06 \times T} & wl \leq 0 \\ 2.33 \times e^{0.16 \times T} & wl > 0 \end{cases} \quad (4)$$

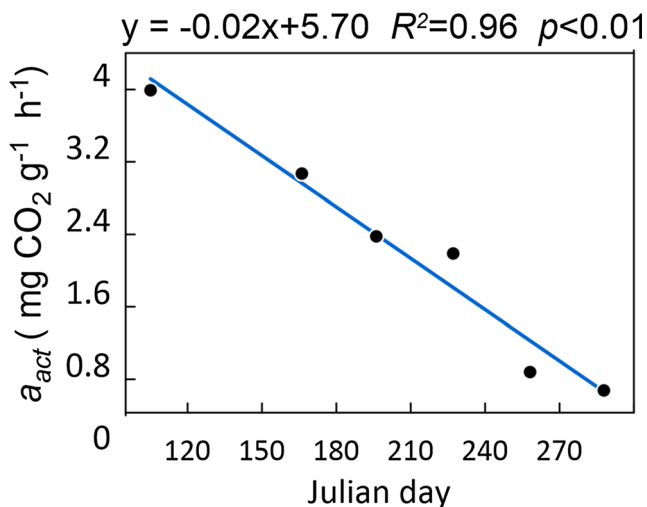


Fig. 11 The relationship between parameter a_{act} and Julian day. The solid dots were calculated a_{act} using each month's data and the line was the fitting curve

where wl was water level and $wl > 0$ indicated the wetland was flooded, and T was air temperature in $^{\circ}\text{C}$.

R_r was calculated according to Fig. 7 and the AGB was the driving variable with the equation of:

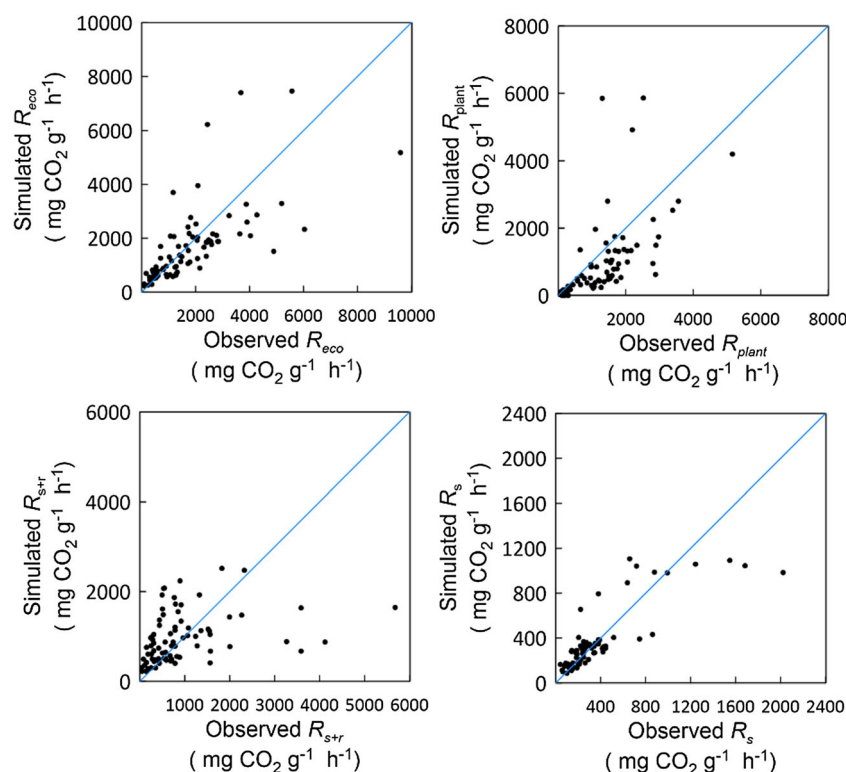
$$R_r = 0.64 \times AGB + 90.5 \quad (5)$$

Using these equations, the ecosystem respiration of *P. australis* wetland could be estimated (Fig. 12). Performance of simulating ecosystem respiration under low flux threshold is better than that under high flux threshold. Therefore, more in-situ accurate flux partitioning observations are still needed to improve the model. The temperature effect of plant respiration under different growing stages is better to be figured out. This simple model could be applied to evaluating ecosystem respiration of similar *Phragmites* wetlands, using above-ground biomass, air temperature, inundation regime, and the date.

Conclusions

The average contribution of plant respiration to ecosystem respiration in the growing seasons was 69% ~ 71%, indicating that the plants could become major source of ecosystem respiration. With the wetland restoration process, the plant biomass increased continuously. The accumulation of plant carbon, resulting in the increase of ecosystem respiration, did not necessarily mean more greenhouse gas emission as living plant could assimilate more CO_2 . More attention should be paid to the seasonal variation of plant growing stage, because it is an easily-ignored factor that controlled the system respiration. The plant respire ability kept decreasing during the growing process from 3.6 $\text{mg CO}_2 \text{ g}^{-1}$ dry mass h^{-1} to 0.2 $\text{mg CO}_2 \text{ g}^{-1}$ dry mass h^{-1} . Soil respiration, however, was temperature dependent but was in different exponential relation according to inundation regime. The soil respiration and its contribution to ecosystem respiration increased when soil surface was not flooded, which meant water level manipulation

Fig. 12 The comparison of simulated and observed components (R_{eco} , R_{plant} , R_{s+r} and R_s) of *P. australis* wetland ecosystem respiration. The lines represented the curve $y = x$



could be a useful way of controlling greenhouse emission. The aboveground/belowground biomass ratio was 1 on seasonal scale, but the underground biomass was accumulated gradually, and finally the underground biomass would be larger than above ground biomass, as the root of *Phragmites* could live more than 1 year while the above ground part did not survive the winters. The gaseous transport from belowground increased with plant biomass and the ecosystem emitted extra 27% CO_2 if plant was detached, leading to more CO_2 emission when the reeds were harvested. To control CO_2 emission and enhance carbon sequestration in wetland restoration, in terms of this study, *Phragmites* with better-developed aerenchyma should be selected and the water level should be kept above ground as long as the inundation would not restrict the growth of plants.

Acknowledgements This study was jointly funded by the National Key R&D Program of China (2016YFE0109600), Ministry of Land and Resources program: “Special foundation for scientific research on public causes” (Grant No. 201111023), National Natural Science Foundation of China (Grant Nos. 41240022 & 40872167), China Geological Survey (Grant Nos. DD20189503, GZH201200503 and DD20160144). Funding for L. Olsson was provided by Sino-Danish Center for Education and Research and the Danish Council for Independent Research – Natural Sciences (Project 4002-00333B) via a grant to HB. Any use of trade, firm, or product names is for descriptive purposes only and does not imply endorsement of the U.S. Government.

We thank Guangming Zhao, Hongming Yuan, Jin Wang, Xigui Ding, Xiongyi Miao, Jin Liu and other staff of our working group for field and

laboratory assistance. We also thank the staff of Reed Institute of Panjin City for the help and convenience they offered.

References

- Achenbach L, Eller F, Nguyen LX, Brix H (2013) Differences in salinity tolerance of genetically distinct *Phragmites australis* clones. *Aob Plants* 5:315–349
- Archer D (2010) *Global carbon cycle*. Princeton Univers. Press
- Armstrong J, Armstrong W (2010) *Phragmites australis*— a preliminary study of soil-oxidizing sites and internal gas transport pathways. *New Phytologist* 108:373–382
- Arora B, Spycher NF, Steefel CI, Molins S, Bill M, Conrad ME, Dong W, Faybishenko B, Tokunaga TK, Wan J (2016) Influence of hydrological, biogeochemical and temperature transients on subsurface carbon fluxes in a flood plain environment. *Biogeochemistry* 127: 1–30
- Bai J, Yu L, Du S, Wei Z, Liu Y, Zhang L, Zhang G, Wang X (2020) Effects of flooding frequencies on soil carbon and nitrogen stocks in river marginal wetlands in a ten-year period. *Journal of Environmental Management* 267:110618
- Berglund Ö, Berglund K (2011) Influence of water table level and soil properties on emissions of greenhouse gases from cultivated peat soil. *Soil Biology and Biochemistry* 43:923–931
- Berglund Ö, Berglund K, Klemmedtsson L (2011) Plant-derived CO_2 flux from cultivated peat soils. *Acta Agriculturae Scandinavica* 61:508–513
- Brix H, Sorrell BK, Schierup H (1996) Gas fluxes achieved by in situ convective flow in *Phragmites australis*. *Aquatic Botany* 54:151–163

- Brix H, Sorrell BK, Lorenzen B (2001) Are *Phragmites*-dominated wetlands a net source or net sink of greenhouse gases? *Aquatic Botany* 69:313–324
- Brix H, Ye S, Laws EA, Sun D, Li G, Ding X, Yuan H, Zhao G, Wang J, Pei S (2014) Large-scale management of common reed, *Phragmites australis*, for paper production: A case study from the Liaohe Delta, China. *Ecological Engineering* 73:760–769
- Carey JC, Tang J, Templar PH, Kroeger KD, Crowther TW, Burton AJ, Dukes JS, Emmett B, Frey SD, Heskell MA (2016) Temperature response of soil respiration largely unaltered with experimental warming. *Proceedings of the National Academy of Sciences of the United States of America* 113:13797–13802
- Ciais P, Sabine C, Bala G, Bopp L, Brovkin V et al (2013) Carbon and other biogeochemical cycles: climate change 2013: the physical science basis. Contribution of working group I to the fifth assessment report of the intergovernmental panel on climate change
- Dawson TE, Tu KP (2009) Partitioning respiration between plant and microbial sources using natural abundance stable carbon isotopes. *Agu Fall Meeting Abstracts*
- Devol AH, Richey JE, Forsberg BR, Martinelli LA (1990) Seasonal dynamics in methane emissions from the Amazon River floodplain to the troposphere. *Journal of Geophysical Research Atmospheres* 95: 16417–16426
- Dyukarev EA (2017) Partitioning of net ecosystem exchange using chamber measurements data from bare soil and vegetated sites. *Agricultural and Forest Meteorology* 239:236–248
- Englender AI (2009) Structure, growth dynamics and biomass of reed (*Phragmites australis*) — a review. *Flora* 204:331–346
- Gao M, Kong F, Xi M, Li Y, Li J (2017) Effects of environmental conditions and aboveground biomass on CO₂ Budget in *Phragmites australis* wetland of Jiaozhou Bay, China. *Chinese Geographical Science* 27:539–551
- Guan B, Yu J, Wang X, Fu Y, Kan X, Lin Q, Han G, Lu Z (2011) Physiological responses of halophyte *Suaeda salsa* to water table and salt stresses in coastal wetland of Yellow River Delta. *Clean – Soil, Air, Water* 39:1029–1035
- Hall S, Hopkins DW (2015) A microbial biomass and respiration of soil, peat and decomposing plant litter in a raised mire. *Plant, Soil and Environment* 61:405–409
- Han GX, Yang LQ, Yu JB, Wang GM, Mao PL, Gao YJ (2012) Environmental effects on net ecosystem CO₂ exchange over a reed (*Phragmites australis*) wetland in the Yellow River estuary, China. *Estuaries and Coasts* 36:401–413
- Hanson P, Edwards N, Garten C, Andrews J (2000) Separating root and soil microbial contributions to soil respiration: a review of methods and observations. *Biogeochemistry* 48:115–146
- Hassink J (1992) Effects of soil texture and structure on carbon and nitrogen mineralization in grassland soils. *Biology and Fertility of Soils* 14:126–134
- Haverd V, Ahlström A, Smith B, Canadell JG (2017) Carbon cycle responses of semi-arid ecosystems to positive asymmetry in rainfall. *Global Change Biology* 23:793–800
- Hirota M, Tang Y, Hu Q, Hirata S, Kato T, Mo W, Cao G, Mariko S (2006) Carbon dioxide dynamics and controls in a deep-water wetland on the Qinghai-Tibetan plateau. *Ecosystems* 9:673–688
- Hu H, Wang D, Li Y, Chen Z, Wu J, Yin Q, Guan Y (2014) Greenhouse gases fluxes at Chongming Dongtan *Phragmites australis* wetland and the influencing factors. *Research of Environmental Sciences* 27: 43–50
- Huang L, Bai J, Wen X, Zhang G, Zhang C, Cui B, Liu X (2020) Microbial resistance and resilience in response to environmental changes under the higher intensity of human activities than global average level. *Global Change Biology* 26:2377–2389
- Ji Y, Zhou G, New T (2009) Abiotic factors influencing the distribution of vegetation in coastal estuary of the Liaohe Delta, Northeast China. *Estuaries and Coasts* 32:937–942
- Juszczak R, Michalak-Galczyńska M, Humphreys E, Olejnik J, Acosta (2013) Ecosystem respiration in a heterogeneous temperate peatland and its sensitivity to peat temperature and water table depth. *Plant and Soil* 366:505–520
- Kim J, Verma SB, Billesbach DP (1999) Seasonal variation in methane emission from a temperate *Phragmites*-dominated marsh: effect of growth stage and plant-mediated transport. *Global Change Biology* 5:433–440
- Krauss KW, Whitbeck JL, Howard RJ (2012) On the relative roles of hydrology, salinity, temperature, and root productivity in controlling soil respiration from coastal swamps (freshwater). *Plant and Soil* 358:265–274
- Lafleur PM, Moore TR, Roulet NT, Frolking S (2005) Ecosystem respiration in a cool temperate bog depends on peat temperature but not water table. *Ecosystems* 8:619–629
- Lee SC, Fan CJ, Wu ZY, Juang JY (2015) Investigating effect of environmental controls on dynamics of CO₂ budget in a subtropical estuarial marsh wetland ecosystem. *Environmental Research Letters* 10:25005–25016
- Liu Y, Reich PB, Li G, Sun S (2011) Shifting phenology and abundance under experimental warming alters trophic relationships and plant reproductive capacity. *Ecology* 92:1201–1207
- Luo H, Huang F, Zhang Y (2003) Space-time change of marsh wetland in Liaohe delta area and its ecological effect. *Journal of Northeast Normal University* 35:100–105
- Ma T, Li X, Bai J, Ding S, Zhou F, Cui B (2019) Four decades' dynamics of coastal blue carbon storage driven by land use/land cover transformation under natural and anthropogenic processes in the Yellow River Delta, China. *Science of the Total Environment* 655:741–750
- Mäkiranta P, Laiho R, Fritze H, Hytönen J, Laine J, Minkkinen K (2009) Indirect regulation of heterotrophic peat soil respiration by water level via microbial community structure and temperature sensitivity. *Soil Biology and Biochemistry* 41:695–703
- Marínmuñiz JL, Hernández ME, Morenocasasola P (2015) Greenhouse gas emissions from coastal freshwater wetlands in Veracruz Mexico: effect of plant community and seasonal dynamics. *Atmospheric Environment* 107:107–117
- Miao Y, Mao R, Song C, Sun L, Wang X, Meng H (2012) Growing season methane emission from a boreal peatland in the continuous permafrost zone of Northeast China: effects of active layer depth and vegetation. *Biogeosciences Discussions* 9:4455–4464
- Mitsch WJ, Gosselink JG (2007) *Wetlands*. Van Nostrand Reinhold Company, New York
- Moomaw WR, Chmura GL, Davies GT, Finlayson CM, Middleton BA, Natali SM, Perry JE, Roulet N, Sutton-Grier AE (2018) *Wetlands in a changing climate: science, policy and management*. *Wetlands*:1–23
- Mukhopadhyay S, Maiti SK (2014) Soil CO₂ flux in grassland, afforested land and reclaimed overburden dumps: a case study. *Land Degradation and Development* 25:216–227
- Nieveen JP, Jacobs CMJ, Jacobs AFG (2010) Diurnal and seasonal variation of carbon dioxide exchange from a former true raised bog. *Global Change Biology* 4:823–833
- Pugh CA, Reed DE, Desai AR, Sulman BN (2018) Wetland flux controls: how does interacting water table levels and temperature influence carbon dioxide and methane fluxes in northern Wisconsin? *Biogeochemistry* 137:15–25
- Rodhe H (1990) A comparison of the contribution of various gases to the greenhouse effect. *Science* 248:1217–1219
- Song H, Liu X (2016) Anthropogenic effects on fluxes of ecosystem respiration and methane in the Yellow River estuary, China. *Wetlands* 36:113–123
- Song C, Xu X, Tian H, Wang Y (2009) Ecosystem-atmosphere exchange of CH₄ and N₂O and ecosystem respiration in wetlands in the Sanjiang plain, northeastern China. *Global Change Biology* 59: 692–705

- Suseela V, Conant RT, Wallenstein MD, Dukes JS (2015) Effects of soil moisture on the temperature sensitivity of heterotrophic respiration vary seasonally in an old-field climate change experiment. *Global Change Biology* 18:336–348
- Townsend SA, Webster IT, Burford MA, Schult J (2018) Effects of autotrophic biomass and composition on photosynthesis, respiration and light utilisation efficiency for a tropical savanna river. *Marine and Freshwater Research* 69:1279
- Unger S (2008) Partitioning ecosystem scale carbon fluxes into photosynthetic and respiratory components with emphasis on dynamics in $\delta^{13}\text{C}$. *Revue Française de Psychanalyse* 71:1203–1215
- Updegraff K, Bridgham SD, Pastor J, Weishampel P, Harth C (2001) Response of CO_2 and CH_4 emissions from peatlands to warming and water table manipulation. *Ecological Applications* 11:311–326
- Vargas R, Allen MF (2008) Environmental controls and the influence of vegetation type, fine roots and rhizomorphs on diel and seasonal variation in soil respiration. *New Phytologist* 179:460–471
- Wang J, Zhao C, Zhao L, Wang X, Qun LI (2018) Response of root morphology and biomass of *Phragmites australis* to soil salinity in inland salt marsh. *Acta Ecologica Sinica*
- White JR, Delaune RD, Roy ED, Corstanje R (2014) Uncertainty in greenhouse gas emissions on carbon sequestration in coastal and freshwater wetlands of the Mississippi River Delta: a subsiding coastline as a proxy for future Global Sea level. AGU Fall Meeting
- Wohlfahrt GAD, Margaret BM, Balzarolo M, Berninger F, Campbell C, Carrara A, Cescatti A, Christensen T, Dore S, Eugster W (2008) Biotic, abiotic, and management controls on the net ecosystem CO_2 exchange of European mountain grassland ecosystems. *Ecosystems* 11:1338–1351
- Wu J, Guan K, Hayek M, Restrepo-Coupe N, Wiedemann KT, Xu X, Wehr R, Christoffersen BO, Miao G, Silva RD (2017) Partitioning controls on Amazon forest photosynthesis between environmental and biotic factors at hourly to interannual timescales. *Global Change Biology* 23:1240–1257
- Xu X, Zou X, Cao L, Zhamangulova N, Zhao Y, Tang D, Liu D (2014) Seasonal and spatial dynamics of greenhouse gas emissions under various vegetation covers in a coastal saline wetland in Southeast China. *Ecological Engineering* 73:469–477
- Yang WB, Yuan CS, Tong C, Yang P, Yang L, Huang BQ (2017) Diurnal variation of CO_2 , CH_4 , and N_2O emission fluxes continuously monitored in-situ in three environmental habitats in a subtropical estuarine wetland. *Marine Pollution Bulletin* 119:289–298
- Ye SY, Krauss KW, Brix H, Wei MJ, Olsson L, Yu XY, Ma XY, Wang J, Yuan HM, Zhao GM (2016) Inter-annual variability of area-scaled gaseous carbon emissions from wetland soils in the Liaohe Delta, China. *PLoS One* 11:e0160612
- Zhou L, Zhou G, Jia Q (2009) Annual cycle of CO_2 exchange over a reed (*Phragmites australis*) wetland in Northeast China. *Aquatic Botany* 91:91–98

Publisher's Note Springer Nature remains neutral with regard to jurisdictional claims in published maps and institutional affiliations.